
This copy is for your personal, non-commercial use only.

If you wish to distribute this article to others, you can order high-quality copies for your colleagues, clients, or customers by [clicking here](#).

Permission to republish or repurpose articles or portions of articles can be obtained by following the guidelines [here](#).

The following resources related to this article are available online at www.sciencemag.org (this information is current as of February 26, 2011):

Updated information and services, including high-resolution figures, can be found in the online version of this article at:

<http://www.sciencemag.org/content/331/6014/189.full.html>

Supporting Online Material can be found at:

<http://www.sciencemag.org/content/suppl/2011/01/12/331.6014.189.DC1.html>

This article **cites 35 articles**, 3 of which can be accessed free:

<http://www.sciencemag.org/content/331/6014/189.full.html#ref-list-1>

This article appears in the following **subject collections**:

Physics

<http://www.sciencemag.org/cgi/collection/physics>

Light-Induced Superconductivity in a Stripe-Ordered Cuprate

D. Fausti,^{1,2*} † R. I. Tobey,^{2,†} § N. Dean,^{1,2} S. Kaiser,¹ A. Dienst,² M. C. Hoffmann,¹ S. Pyon,³ T. Takayama,³ H. Takagi,^{3,4} A. Cavalleri^{1,2*}

One of the most intriguing features of some high-temperature cuprate superconductors is the interplay between one-dimensional “striped” spin order and charge order, and superconductivity. We used mid-infrared femtosecond pulses to transform one such stripe-ordered compound, nonsuperconducting $\text{La}_{1.675}\text{Eu}_{0.2}\text{Sr}_{0.125}\text{CuO}_4$, into a transient three-dimensional superconductor. The emergence of coherent interlayer transport was evidenced by the prompt appearance of a Josephson plasma resonance in the c -axis optical properties. An upper limit for the time scale needed to form the superconducting phase is estimated to be 1 to 2 picoseconds, which is significantly faster than expected. This places stringent new constraints on our understanding of stripe order and its relation to superconductivity.

High-temperature cuprate superconductors are synthesized by chemically doping the parent compound, an antiferromagnetic Mott insulator. An example of a parent compound is La_2CuO_4 , which turns into an unconventional metal as holes are doped into its CuO_2 planes by substitution of La by Ba or Sr. $\text{La}_{2-x}(\text{Ba}/\text{Sr})_x\text{CuO}_4$ becomes superconducting for $x > 0.05$, reaching the highest critical temperatures near $x = 0.16$. The $x = 1/8$ compound deserves special attention, because it hosts one-dimensional (1D) modulations of charge and spin (1) and exhibits sharp reduction in critical temperature T_c (superconducting transition temperature). In the Ba-doped system, these “stripes” become static, enhanced by the buckled Cu-O planes in the so-called low-temperature tetragonal (LTT) phase (2, 3). Static stripes, LTT phases (4), and suppressed superconductivity are also detected in $\text{La}_{1.48}\text{Nd}_{0.4}\text{Sr}_{0.12}\text{CuO}_4$ (5, 6) and $\text{La}_{1.675}\text{Eu}_{0.2}\text{Sr}_{0.125}\text{CuO}_4$ (LESCO_{1/8}) (7). Figure 1 shows a schematic phase diagram of $\text{La}_{1.8-x}\text{Eu}_{0.2}\text{Sr}_x\text{CuO}_4$, in which T_c is strongly reduced in the stripe region, for all doping values below $x = 0.2$ (8, 9).

The transition between a doped Mott insulator and a superconductor has long been at the heart of research into cuprate superconductivity. Virtually all studies have explored this transition by changing static doping or by adiabatically tuning an external parameter, such as pressure, to

demonstrate that superconductivity can be restored if the equilibrium crystallographic structure is perturbed (10).

We dynamically perturbed the nonsuperconducting LESCO_{1/8} with mid-infrared (mid-IR) radiation (11, 12), inducing superconductivity on the ultrafast time scale. Optical excitation in the visible or near-IR has been used in the past to study (13–18), and sometimes even enhance (19), superconductivity. However, in all these cases, superconductivity could be achieved only after the relaxation of hot incoherent carriers back to the ground state and was not triggered directly by the light field.

Nonsuperconducting LESCO_{1/8}, held at a base temperature of 10 K, was excited with 15- μm -wavelength pulses (80 meV of photon energy), made resonant with an in-plane, near-600 cm^{-1} , Cu-O stretch. The time-dependent intensity reflectivity, $R = I_{\text{refl}}/I_{\text{inc}}$ (refl, reflected; inc, incident), was measured in the near-IR (1.5 eV), a photon energy at which the optical properties are indirectly related to the appearance of superconductivity (20–22). A prompt reflectivity change, remaining constant up to the longest time delays probed (100 ps), was observed (Fig. 2). Photoexcitation with the electric field polarized orthogonal to the planes resulted in only a small reflectivity change during the pump pulse and no long-lived response.

The long-lived photoinduced state of LESCO_{1/8}, can be shown to be superconducting by time-resolved terahertz spectroscopy. At equilibrium, superconductivity in cuprates is reflected in the appearance of a Josephson plasma resonance (JPR) in the c -axis terahertz optical properties. This is a general feature of cuprate superconductors (23–25), well understood by noting that 3D superconductivity in these compounds can be explained by Josephson coupling between capacitively coupled stacks of quasi-2D superconducting layers (26). This effect is shown in Fig. 3A for optimally doped $\text{La}_{1.84}\text{Sr}_{0.16}\text{CuO}_4$. A plasma edge in the reflectance appears near 60 cm^{-1} when the temperature is reduced below $T_c = 38$ K.

Figure 3C reports mid-IR pump, terahertz reflectance-probe measurements in nonsuperconducting LESCO_{1/8}. The equilibrium electric field reflectance, as in other striped cuprates (27),

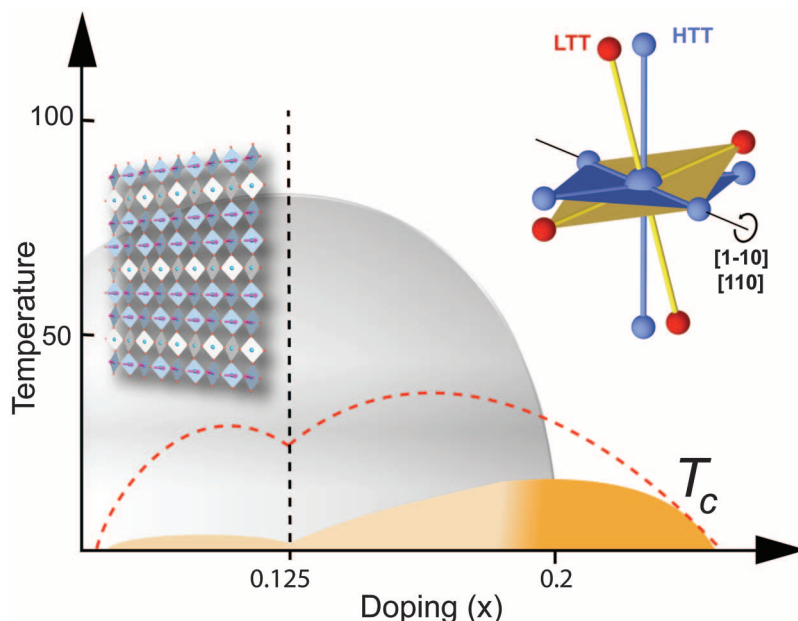


Fig. 1. Schematic phase diagram for $\text{La}_{1.8-x}\text{Eu}_{0.2}\text{Sr}_x\text{CuO}_4$. Superconductivity (yellow area) is quenched at all doping levels (gray area) below 0.2, emerging only at very low temperatures. At 0.125 doping, a static 1D modulation of charges and spins, the stripe state, emerges in the planes. This stripe phase (left inset) is associated with a LTT distortion, in which the oxygen octahedra in the crystal are tilted (right inset). The red dashed curve marks the boundary for superconductivity in compounds of the type $\text{La}_{2-x}\text{Sr}_x\text{CuO}_4$, in which the LTT structural modulation is less pronounced.

¹Max Planck Research Department for Structural Dynamics, University of Hamburg—Centre for Free Electron Laser Science—Hamburg, Germany. ²Department of Physics, Clarendon Laboratory, University of Oxford, Oxford, UK. ³Department of Advanced Materials Science, University of Tokyo, Tokyo, Japan. ⁴IKEN Advanced Science Institute, Hirosawa 2-1, Wako 351-0198, Japan.

*To whom correspondence should be addressed. E-mail: andrea.cavalleri@mpsd.cfel.de (A.C.); daniele.fausti@mpsd.cfel.de (D.F.)

†These authors contributed equally to this work.

‡Present address: University of Trieste, Trieste, Italy.

§Present address: Physics Division, Brookhaven National Laboratory, Upton, NY, USA.

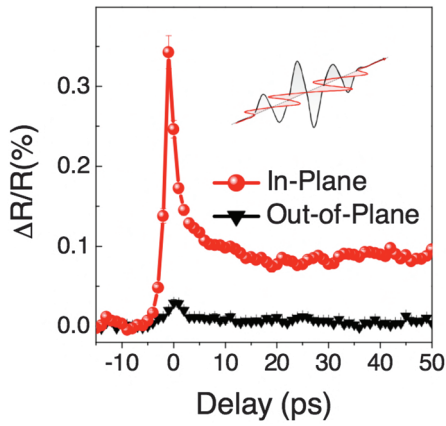
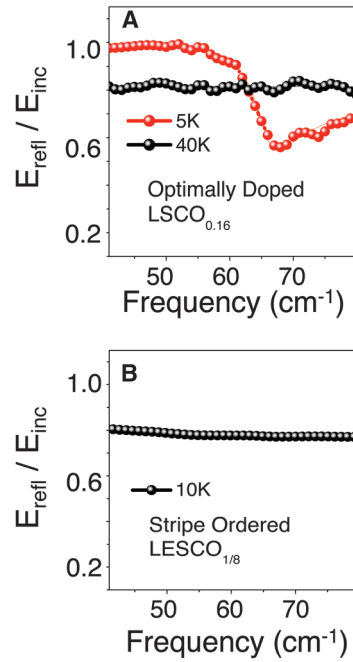


Fig. 2. Time-dependent 800-nm intensity reflectivity changes after excitation with IR pulses at $16\ \mu\text{m}$ wavelength and $\sim 1\text{mJ}/\text{cm}^2$ intensity. Photoexcitation along the Cu-O planes results in the appearance of a long-lived meta-stable phase lasting longer than 100 ps. Excitation with the electric field polarized orthogonal to the Cu-O plane results in minimal reflectivity changes.

exhibits a featureless terahertz response reminiscent of that of $\text{LSCO}_{0.16}$ above T_c (Fig. 3B). Five picoseconds after excitation, a plasma edge at a frequency comparable to that of the $\text{LSCO}_{0.16}$ JPR is observed, indicating the emergence of coherent transport in the c axis. This is the most important observation of our work, evidencing ultrafast photoinduced superconductivity in $\text{LSCO}_{1/8}$.

The measured change in the absolute terahertz field reflectance is less than 1%, which is suggestive of an incomplete transformation of the probed volume. This is well explained by noting that the pump field penetration depth is about 200 nm, whereas the terahertz probe samples a depth of nearly $10\ \mu\text{m}$. The raw data of Fig. 3C was processed assuming a total terahertz reflectance resulting from a homogeneously transformed surface layer and an unperturbed bulk beneath. Relying on the knowledge of both amplitude and phase of the static and transient field reflectance, we could isolate the real and imaginary part of the time- and frequency-dependent optical conductivity $\sigma_1(\omega, \tau) + i\sigma_2(\omega, \tau)$ in the surface layer. In Fig. 4, we plot the imaginary part $\sigma_2(\omega, \tau)$, after subtracting a component originating from higher-frequency oscillators, which are also perturbed by photoexcitation and give a negative contribution to the conductivity change (28). The imaginary time-dependent conductivity $\sigma_2(\omega, \tau)$ acquires a $1/\omega$ frequency dependence immediately after excitation. A divergent imaginary conductivity at low frequencies is a defining characteristic of a superconductor. The real part $\sigma_1(\omega) = \pi/2(n_s e^2/m^*)\delta(0)$ reflects vanishing DC resistivity, and $\sigma_2(\omega) = n_s e^2/m^* \omega$ is connected to the diamagnetic response, and to the Meissner effect as $\omega \rightarrow 0$ (29). Here n_s is the



In the equilibrium low-temperature superconducting state, a Josephson plasma edge is clearly visible, reflecting the appearance of coherent transport. This edge is fitted with a two-fluid model (continuous line). Above T_c , incoherent ohmic transport is reflected in a featureless conductivity. **(B)** Static c -axis reflectance of $\text{LSCO}_{1/8}$ at 10 K. The optical properties are those of a nonsuperconducting compound down to the lowest temperatures. **(C)** Transient c -axis reflectance of $\text{LSCO}_{1/8}$, normalized to the static reflectance. Measurements are taken at 10 K, after excitation with IR pulses at $16\ \mu\text{m}$ wavelength. The appearance of a plasma edge at $60\ \text{cm}^{-1}$ demonstrates that the photoinduced state is superconducting.

superfluid density, e is the electron charge, and m^* is the electron effective mass (30). The quantity $\omega\sigma_2(\omega \rightarrow 0^*, \tau)$ (31), defined as the low-frequency limit of the measured terahertz transient for various pump-probe time delays, provides a measure of the formation time of the superconducting state (Fig. 4B). The prompt appearance of finite superconducting density, overshooting before relaxing into a plateau at a 5-ps time delay, reflects the transition dynamics between the striped state and the 3D superconductor. The temperature dependence of $\sigma_2(\omega, \tau)$, for time delays $\tau = 5$ ps shows that the signatures of the transient superconducting state are lost above a base temperature of 20 K, at least for the $1\ \text{mJ}/\text{cm}^2$ excitation fluence used here (Fig. 4C).

In Fig. 4D we plot the wavelength-dependent susceptibility for photoinduced superconductivity, operationally defined as the inverse of the fluence F_{sat} at which the photoinduced optical properties start saturating (see supporting online material). The key observation is that the photosusceptibility has a pronounced peak at the frequency of the phonon. In comparison, at the same frequency, the reflectivity and the extinction coefficient change only marginally. As shown in Fig. 4D, the photosusceptibility (red dots) follows the phonon-resonance line shape (dashed curve), plotted as a “partial” extinction coefficient α_{phonon} and associated with a single oscillator extracted from a Drude-Lorentz fit of the

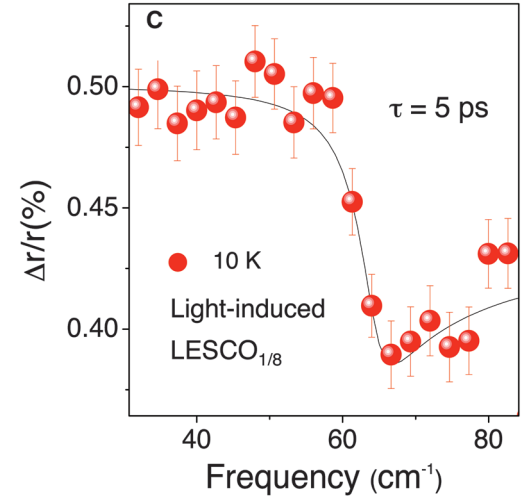


Fig. 3. **(A)** Static c -axis electric field reflectance ($r = E_{\text{refl}}/E_{\text{inc}}$) of $\text{LSCO}_{0.16}$, measured at a 45° angle of incidence above (black dots) and below (red dots) $T_c = 38\ \text{K}$. Here field reflectances $r = E_{\text{refl}}/E_{\text{inc}}$ are measured, as opposed to intensity reflectivities in the near-IR, because the time domain detection scheme for short terahertz transients is sensitive to the electric field.

broadband reflectivity (28). This observation suggests that direct coupling to the crystal structure may be responsible for the ultrafast transition into the superconducting phase.

The detailed microscopic pathway that leads to the superconducting state deserves further discussion. As a working hypothesis, it is helpful to relate our work to recent studies in striped cuprates, in which evidence for low-temperature 2D superconductivity was found (32). A plausible explanation for the decoupling between different striped planes follows directly from the crystallographic structure of the LTT phase (33), in which stripes of neighboring planes are oriented in perpendicular directions, whereas the next-nearest planes exhibit a shift of a half stripe period. This leads to a superconducting order that is in antiphase between stripes within each plane, and to canceling of the lowest-order Josephson coupling between planes (34).

In our experiment, the Josephson effect is reestablished when mid-IR pulses perturb the stripe state, which we attribute to a direct distortion of the LTT structure by the mid-IR radiation. The data of Fig. 4B provides a rise time for the formation of the superconducting state $\tau_{\text{SC}} < 1$ to 2 ps, limited by the temporal resolution of our measurement. This is a surprisingly short time scale, and it is difficult to imagine how mutually incoherent planes could synchronize so rapidly. At 5 K, only the 100-GHz modes are

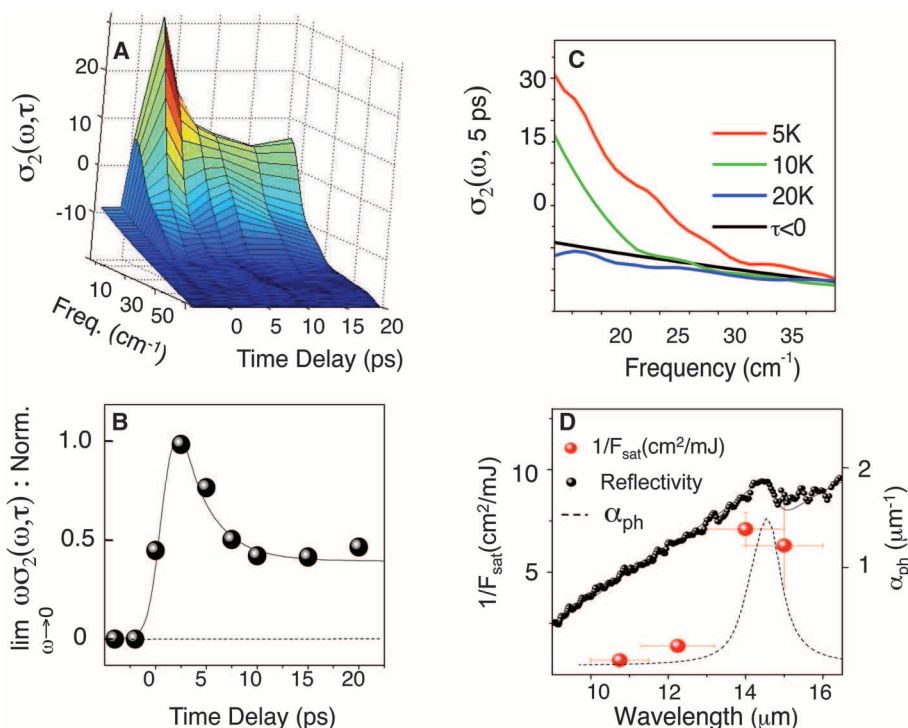


Fig. 4. (A) Time- and frequency-dependent imaginary conductivity $\sigma_2(\omega, \tau)$ of $\text{LESCO}_{1/8}$ at 10 K after excitation with IR pulses at 16 μm wavelength. The appearance of a $1/\omega$ dispersion demonstrates that the system becomes superconducting on the shortest time scales accessible here. (B) Time-dependent plot of the normalized function $\omega\sigma_2(\omega \rightarrow 0, \tau)$, proportional to the condensate density. (C) Transient measurement of the imaginary conductivity $\sigma_2(\omega, 5 \text{ ps})$, demonstrating that for the fluence used here ($< 1 \text{ mJ}/\text{cm}^2$), photoinduced superconductivity can only be induced for base temperatures $T_b < 20 \text{ K}$. (D) Photosusceptibility, defined as the inverse of the saturation fluence plotted as a function of wavelength (red dots) compared to the reflectivity (black dots) of $\text{LESCO}_{1/8}$ measured in the ab plane. By means of a Drude-Lorentz fitting, the partial extinction coefficient for the α_{phonon} is extracted (dashed curve) and compared to the photosusceptibility.

thermally populated, and no spontaneous fluctuation could drive a process on time scales shorter than 10 ps.

This short time scale supports a picture in which information about the superconducting state is already present in the system before excitation. Indeed, if the planes were simply anticorrelated at equilibrium, recoupling could occur on a time scale needed to change the interplane order parameter phase difference, reestablishing the Josephson effect. This time scale may be very fast, commensurate with the Josephson plasmon period $T_{\text{JPR}} \sim 600 \text{ fs}$.

The temperature at which photoinduced superconductivity disappears is near 10 to 20 K, significantly below $T_c = 35 \text{ K}$ in $\text{LSCO}_{0.16}$ and similar to the Berezinskii-Kosterlitz-Thouless temperature ($T_{\text{BKLT}} = 16 \text{ K}$) found from transport measurements in other striped compounds (3). One can speculate that the disappearance of 2D fluctuations for $T < T_{\text{BKLT}}$ may be a necessary condition for photoinduced recoupling.

At the earliest time scales, a key question relates to the fate of stripe order once the Josephson coupling has been established. Time-resolved measurements of the stripe order, possible by extending

soft x-ray scattering techniques (35) to the time domain, could clarify whether superconductivity emerges only in response to stripe melting, or, in contrast, the two can coexist.

Our measurements have not probed the dynamics beyond 100-ps time delays, although no relaxation was found on that time scale. We can thus deduce that the transient superconducting phase does not relax back for many nanoseconds, possibly more. The long lifetime can be understood by noting that once the 3D superconducting state is formed, the new broken symmetry leads to rigidity and to the formation of a kinetic barrier, which stabilizes the superconducting state.

The present paper has demonstrated that light can be used to affect phase competition in the underdoped cuprates, allowing for the emergence of a transient superconducting state at temperatures where the striped phase is the true ground state of the system. Similar photo-stimulation could be used to explore a broader region of the underdoped phase diagram, especially at doping levels and temperatures for which the electronic structure is already gapped (36) and signatures of quantum coherence are already

present, but 3D superconductivity is not established (37).

References and Notes

1. J. Zaenen, O. Gunnarsson, *Phys. Rev. B* **40**, 7391 (1989).
2. T. Suzuki, T. Fujita, *Physica C* **159**, 111 (1989).
3. M. K. Crawford *et al.*, *Phys. Rev. B* **44**, 7749 (1991).
4. M. Fujita, H. Goka, K. Yamada, M. Matsuda, *Phys. Rev. Lett.* **88**, 167008 (2002).
5. J. Tranquada, B. J. Sternlieb, J. D. Axe, Y. Nakamura, S. Uchida, *Nature* **375**, 561 (1995).
6. Y. Nakamura, S. Uchida, *Phys. Rev. B* **46**, 5841 (1992).
7. J. Fink *et al.*, *Phys. Rev. B* **79**, 100502 (2009).
8. H. H. Klauss *et al.*, *Phys. Rev. Lett.* **85**, 4590 (2000).
9. Suryadjaya *et al.*, *Physica C* **426**, 402 (2005).
10. N. Takeshita, T. Sasagawa, T. Sugioka, Y. Tokura, H. Takagi, *J. Phys. Soc. Jpn.* **73**, 1123 (2004).
11. M. Rini *et al.*, *Nature* **449**, 72 (2007).
12. R. I. Tobey, D. Prabhakaran, A. T. J. Boothroyd, A. Cavalleri, *Phys. Rev. Lett.* **101**, 197404 (2008).
13. R. D. Averitt *et al.*, *Phys. Rev. B* **63**, 140502 (2001).
14. J. Demsar, B. Podobnik, V. Kabanov, T. Wolf, D. Mihailovic, *Phys. Rev. Lett.* **82**, 4918 (1999).
15. R. A. Kaindl *et al.*, *Science* **287**, 470 (2000).
16. N. Gedik, D. S. Yang, G. Logvenov, I. Bosovic, A. H. Zewail, *Science* **300**, 1410 (2003).
17. L. Perfetti *et al.*, *Phys. Rev. Lett.* **99**, 197001 (2007).
18. A. Pashkin *et al.*, *Phys. Rev. Lett.* **105**, 067001 (2010).
19. G. Nieva *et al.*, *Appl. Phys. Lett.* **60**, 2159 (1992).
20. G. P. Segre *et al.*, *Phys. Rev. Lett.* **88**, 137001 (2002).
21. N. Gedik *et al.*, *Phys. Rev. Lett.* **95**, 117005 (2005).
22. C. Giannetti *et al.*, *Phys. Rev. B* **79**, 224502 (2009).
23. V. Z. Kresin, H. Morawitz, *Phys. Rev. B* **37**, 7854 (1988).
24. H. A. Fertig, S. Das Sarma, *Phys. Rev. Lett.* **65**, 1482 (1990).
25. K. Tamasaku, Y. Nakamura, S. Uchida, *Phys. Rev. Lett.* **69**, 1455 (1992).
26. N. Basov, T. Timusk, B. Dabrowski, J. D. Jorgensen, *Phys. Rev. B* **50**, 3511 (1994).
27. T. Tajima, T. Noda, H. Eisaki, S. Uchida, *Phys. Rev. Lett.* **86**, 500 (2001).
28. See supporting material on Science Online.
29. J. F. Annett, *Superconductivity, Superfluids and Condensates* (Oxford Master Series in Condensed Matter Physics, Oxford, 2004).
30. D. N. Basov, T. Timusk, *Rev. Mod. Phys.* **77**, 721 (2005).
31. N. Basov *et al.*, *Science* **283**, 49 (1999).
32. Q. Li, M. Hücker, G. Gu, A. Tselik, J. Tranquada, *Phys. Rev. Lett.* **99**, 067001 (2007).
33. M. von Zimmermann *et al.*, *Europhys. Lett.* **41**, 629 (1998).
34. E. Berg *et al.*, *Phys. Rev. Lett.* **99**, 127003 (2007).
35. P. Abbamonte *et al.*, *Nat. Phys.* **1**, 155 (2005).
36. T. Timusk, B. Statt, *Rev. Mod. Phys.* **62**, 61 (1999).
37. Z. A. Xu, N. P. Ong, Y. Wang, T. Kakeshita, S. Uchida, *Nature* **406**, 486 (2000).
38. This research was supported by a 2004 European Young Investigator Award, by core support from the Max Planck Society and the University of Hamburg, and by a Japanese Ministry of Education, Culture, Sports, Science and Technology (MEXT) Grant-in-Aid for Scientific Research (S) (19104008).

Supporting Online Material

www.sciencemag.org/cgi/content/full/331/6014/189/DC1
Materials and Methods
Figs. S1 to S3

2 September 2010; accepted 7 December 2010
10.1126/science.1197294